Arabian Journal of Geosciences (2022) 15:1659
https://doi.org/10.1007/s12517-022-10927-4

ORIGINAL PAPER

# Seasonal variability of hydrography off the east coast of Qatar, central Arabian Gulf

**Ebrahim M. A. S. Al-Ansari[1] · Y. Sinan Husrevoglu[1,2] · Oguz Yigiterhan[1] · Nabiha Youssef[1,3,4] · Ibrahim A. Al-Maslamani[5] · Mohamed A. Abdel-Moati[6] · Ahmad J. Al-Mohamedi[7] · Valliyil Mohammed Aboobacker[1] · Ponnumony Vethamony[1]**

Received: 21 February 2022 / Accepted: 13 October 2022 / Published online: 4 November 2022
© The Author(s) 2022

## Abstract

Seasonal variability of hydrography along a nearshore-offshore transect in the eastern part of the EEZ of Qatar has been analyzed using in situ measurements carried out during 5 different months. The study reveals distinct features in temperature, salinity, density, dissolved oxygen (DO), and chlorophyll fluorescence. The sea surface temperature (SST) varies from nearshore to offshore with a positive gradient during January, June, and August, of the order of 1.0–2.0 °C, and with a negative gradient during October and April, of the order of 1.0 °C. Thermal stratification began in June, reached a well-defined thermocline with a vertical difference in temperature of about 10 °C during August, and started to de-stratify during October. The low salinity and low-density inflow of IOSW is evident in the surface layer of the middle of the transect during August, which has enriched the DO in the surface layer up to 20 m depth, while hypoxia prevailed below 50 m depth. The lowest chlorophyll fluorescence was measured in April 2013 (~ 1.0 µg $l^{-1}$), moderate in June 2013 (~ 1.5 µg $l^{-1}$), and relatively high in August 2013 (~ 6.0 µg $l^{-1}$).

**Keywords** Hydrography · Biogeochemistry · Ocean stratification · Qatar · Arabian Gulf

## Introduction

The Arabian/Persian Gulf (hereafter the "Gulf") is a semi-enclosed, shallow marginal sea connected to the Arabian Sea through the Strait of Hormuz (Fig. 1). It is a hypersaline and warmest marine area in the world, where evaporation exceeds precipitation (Al-Ansari et al. 2015). The evaporation rate estimated in the Gulf is 1.4–2.1 m $year^{-1}$ (Xue and Eltahir, 2015), while the precipitation and river run-off are in the range of 0.03–0.11 and 0.1–0.46 m $year^{-1}$, respectively (Al Senafi and Anis 2015; Al-Mazroui et al. 2012). Recent studies indicate that harmful environmental impacts of anthropogenic origin in the Gulf increase in frequency (Al-Ansari et al. 2015; Feary et al. 2011; Sheppard et al. 2010; Al-Ansi et al. 2002). Besides the increasing natural and anthropogenic stresses that affect the nearshore regions, the water mass exchanges and circulation greatly help to maintain stable conditions in most of the Gulf. For instance, Ibrahim et al. (2020) identified that the Gulf basin salinity is relatively stable and resilient to the existing brine discharges from the desalination plants around the Gulf. However, the impacts of brine charges on the marine ecosystem are crucial

Responsible Editor: Zhihua Zhang

Abdel-Moati has passed away during the preparation of this study.

✉ Ebrahim M. A. S. Al-Ansari
isalansari@qu.edu.qa

[1] Environmental Science Center, Qatar University, P.O. Box: 2713, Doha, Qatar

[2] Middle East Technical University, Institute of Marine Sciences, P.O.Box 28, 33731 Erdemli-Mersin, Turkey

[3] National Institute of Oceanography and Fisheries, Cairo, Egypt

[4] Oceanography Department, Faculty of Science, Alexandria University, Alexandria, Egypt

[5] Office of Vice President for Research and Graduate Studies, Qatar University, P.O. Box: 2713, Doha, Qatar

[6] Ministry of Municipality and Environment, Doha, Qatar

[7] Department of Biological and Environmental Sciences, Qatar University, P.O. Box: 2713, Doha, Qatar

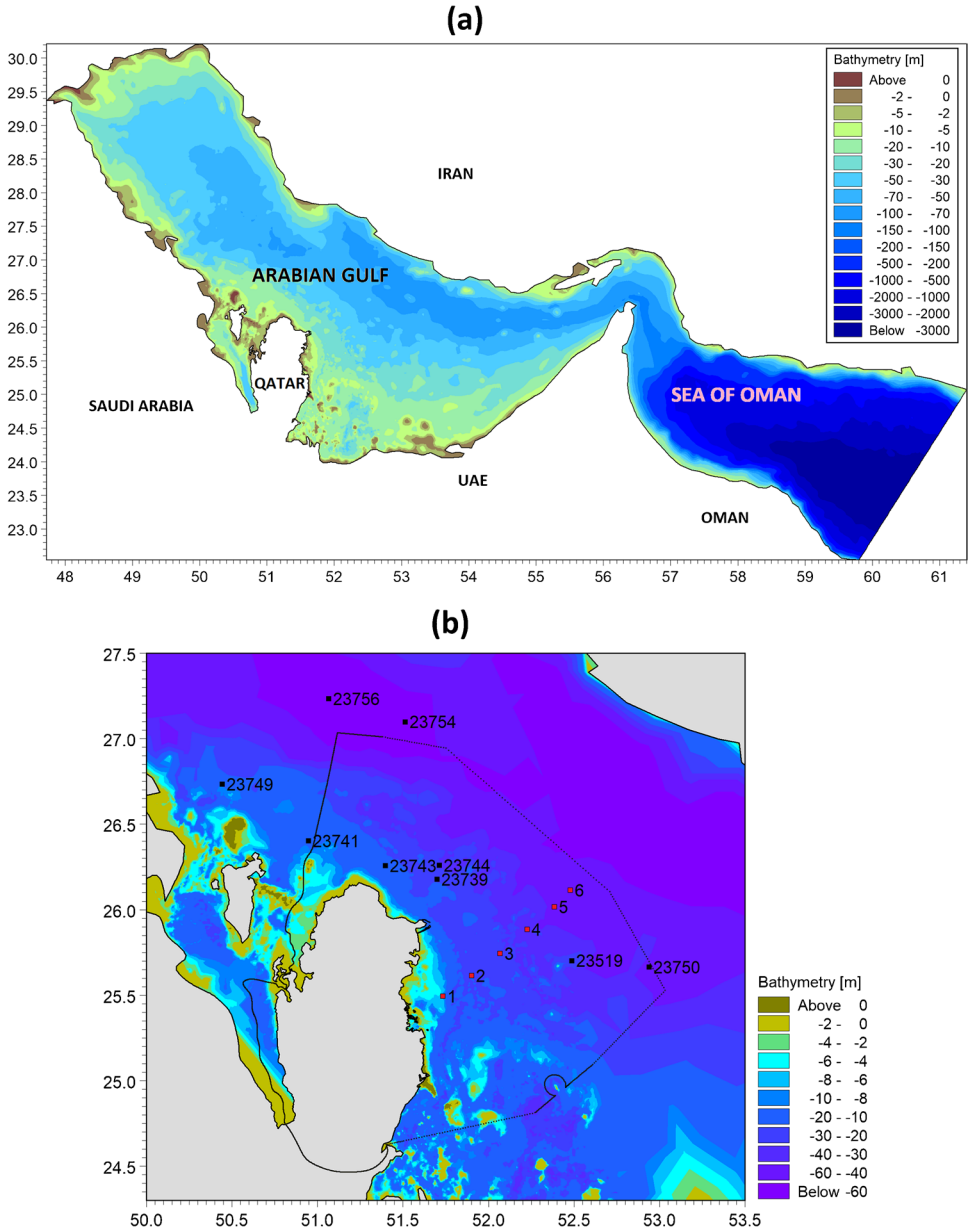


**Fig. 1** **a** Geographical map and C-MAP bathymetry of the Arabian Gulf and **b** EEZ of Qatar (dotted lines indicate the boundary). Red dots numbering 1 to 6 are the sampling stations. Black dots numbered in 5 digits are the Coriolis drifting buoy positions during the study period

in the nearshore waters of the Gulf (Hosseini et al. 2021; Joydas et al. 2015).

The basin-scale circulations, seawater properties, and water masses were investigated in the Gulf (Al-Shehhi et al. 2021; Campos et al. 2020; Azizpour et al. 2014; Yao and Johns, 2010a, b; Swift and Bower, 2003; Reynolds, 1993). The exchange of water masses between the Gulf and the Arabian Sea maintains a stable salt budget in the Gulf (Johns et al. 2003). The high-saline and well-oxygenated Persian Gulf Water (PGW) enters the Arabian Sea through the Strait of Hormuz, ventilating the world's thickest oxygen minimum zone (OMZ), and flows further down into the Indian Ocean (Lachkar et al. 2019). The outflow water during the first half of the year mostly originates from the southern Gulf coast, while that during the second half is mainly transported from the northwestern Gulf (Lorenz et al. 2020). Traces of PGW have been identified in the northwestern Indian Ocean and Bay of Bengal, indicating that the saltier PWG is strong enough to impact the biological activity in these regions (L'Hégaret et al. 2021; Sheehan et al. 2020). Whereas the low-saline Indian Ocean Surface Water (IOSW) flows into the Gulf through the Strait of Hormuz, which is more evident during summer (Kampf and Sadrinasab, 2006). The distribution of water masses and the formation of a strong pycnocline during summer reflect the combined influence of horizontal and vertical spreading of low-salinity surface inflow and excessive atmospheric heating (Al-Ansari et al.

2015). The presence of IOSW has been identified in the deep waters of the Exclusive Economic Zone (EEZ) of Qatar (Rakib et al. 2021; Elobaid et al. 2022). Horizontal and vertical gradients in temperature, salinity, and density are evident in the Gulf basin during summer, caused by the extreme surface heating (Pous et al. 2015; Kampf and Sadrinasab, 2006). However, vertical gradients are diminished during the winter due to well-mixing by the winter shamal winds (Al Azhar et al. 2016).

The biogeochemistry and ecosystems of the Gulf are experiencing massive changes in recent years, caused by a reduction in river runoff in the north and an increase in nutrient loading from the urban areas (Al-Yamani and Naqvi, 2019). Increasing sea surface temperature (SST) in response to global warming is another factor that influences the physical and biogeochemical distribution in the Gulf (Noori et al. 2019; Strong et al. 2011). The phytoplankton biomass (chlorophyll *a*) is reported to decrease from approximately 94 μg $l^{-1}$ in the Shatt Al-Arab estuary in the north to about 2–4 μg $l^{-1}$ around Qatar and off the Abu Dhabi coast (Al-Naimi, et al. 2017; Mezhoud et al. 2016; Quigg et al. 2013). Low biomass and productivity in the Gulf are attributed to its shallow nature, moderate to strong wind and current regimes, and well-mixed water column driven by geomorphology and physical dynamics (Al-Ansari et al. 2015; Jones, 1985). Due to excess respiration and microbial decomposition in the subsurface (depth > 45 m), dissolved oxygen (DO) concentration in the deepest part of the central Gulf and on the Iranian side of the Strait of Hormuz decreases throughout the summer and reaches hypoxic levels by early autumn (Saleh et al. 2021; Al-Ansari et al. 2015). Short episodes of summer hypoxia were identified at Dhabiya Reef in the southern Gulf (De Verneil et al. 2021) and Sulaibikhat Bay in Kuwait (Al-Mutairi et al. 2014).

The physical and biogeochemical characteristics of the Gulf are highly complex due to bathymetric-anthropogenic-climatic interactions. While climatic features are regional in nature, bathymetric and anthropogenic influences are mostly localized. Although basin-scale features have been explored to some extent, focused studies pertaining to the localized physical-biogeochemical interactions and features are very limited, especially in the EEZ of Qatar. The summer hypoxia explored in the central Gulf (Al-Ansari et al. 2015) and the studies carried out on the hydrography and biogeochemistry (Elobaid et al. 2022; Rakib et al. 2021) point out the necessity of having further investigations in the EEZ of Qatar. The main constraint on this is the lack of measurements in this region. The present study utilizes seasonal datasets measured on a transect off the east coast of Qatar and the available Coriolis Ocean Data to investigate the distribution and seasonal variability of temperature, salinity, density, DO, and chlorophyll fluorescence in the water column.

## Area of study

The Gulf, located between the latitudes 24.0°–30.5° N and the longitudes 48.0°–56.5° E, is an extension of the Arabian Sea (Indian Ocean) and covers an ocean area of about 241,000 $km^2$ (Fig. 1). It has a length of 990 km, a width ranging from 56 to 340 km, a maximum depth of approximately 110 m, and an average depth of 36 m (Sadrinasab and Kämpf, 2004). The deeper areas of the Gulf are located along the Iranian coast, while broad shallow regions with depths of less than 35 m are located along the Arabian coast. Winds of various scales and directions dominate the Gulf, with the northwesterly shamal winds, northeasterly/easterly nashi winds, and southeasterly/southerly kaus winds having a significant influence on sea surface dynamics (Aboobacker et al. 2021a,b c; Veerasingam et al. 2020a, b; Perrone 1979).

The EEZ of Qatar is in the central Gulf, covering 14% of the total area of the basin (Al-Qaradawi et al. 2015). The EEZ is relatively larger and deeper off the east and north coasts of Qatar, bordering Iranian and UAE waters (Fig. 1b). The west part of the EEZ is very narrow and shallow and border on Bahrain and Saudi Arabia.

## Data and methods of analysis

This study uses the hydrographic and biogeochemical data measured at 6 stations along a 105-km transect off the east coast of Qatar in 5 cruises during 2012–2013 (Fig. 1; Table 1) utilizing the R/V Janan (owned and operated by Qatar University). Samples were collected during October 2012, January 2013, April 2013, June 2013, and August 2013. The transect, which ends at the Qatari marine border, traverses more than half of the linear distance between Doha and the Iranian coast, thus providing a reasonable representation of hydrographic distributions across this relatively wider part of the Gulf. Although limited to a single transect extending from the coast to the center of

**Table 1** Geographical coordinates of sampling locations and water depths

| Station ID | Longitude (°E) | Latitude (°N) | Depth (m) |
|---|---|---|---|
| 1 | 51.733 | 25.494 | 11 |
| 2 | 51.901 | 25.615 | 24 |
| 3 | 52.067 | 25.744 | 30 |
| 4 | 52.226 | 25.885 | 39 |
| 5 | 52.384 | 26.017 | 53 |
| 6 | 52.477 | 26.114 | 55 |

the Gulf, this dataset is the first of its kind, and it has never been utilized before to investigate the seasonal variability of water column structure.

The profiling of temperature and salinity for every 1.0 m depth was carried out using the SBE-25 plus CTD system in October 2012 and using the SBE-911plus CTD for the remaining 4 cruises conducted in 2013. In October 2012 and January 2013, discrete sampling was carried out for DO using SBE-32 Carousel fitted with 12-l Niskin bottles. DO samples were analyzed for concentration and saturation onboard within a few hours of collection using the titrimetric method (Winkler 1888). This method was used earlier in the EEZ of Qatar (Rakib et al. 2021; Al-Ansari et al. 2015) and other parts of the Gulf (Naqvi 2021; Saleh et al. 2021) However, in April 2013, the CTD system was fitted with new sensors for in situ DO (SBE-43) and chlorophyll fluorescence (WET Labs ECO-FL-NTU-RT-D) measurements. These sensors were well calibrated (Janzen et al. 2008). Therefore, we relied on the pre-established accuracy of the sensors, since a comparison between the sensor and titration data has not been carried out. Recently, a luminescent DO sensor (Hach IntelliCal LDO101) data in the Iranian waters of the Gulf was verified well with the titration results (Saleh et al. 2021). Ocean Data View (ODV) was used to analyze and visualize bin-averaged downcast CTD data and laboratory DO data (Schlitzer 2015).

The in situ data in the Gulf is sparse, especially in the EEZ of Qatar. We have explored the global resources of in situ data within the study region and were able to identify a few data points of Coriolis Ocean products (Table 2). The Coriolis Ocean Dataset provides operational oceanography data around the world oceans (Tanguy et al. 2019). This dataset contains observations assimilated from different sources such as autonomous platforms (Argo profilers, fixed moorings, gliders, drifters, sea mammals) and vessels (CTDs, XBTs, ferryboxes).

Surface wind data in the nearshore and offshore regions along the transect has been obtained from the European Centre for Medium-Range Weather Forecasts (ECMWF) product, ERA5. ERA5 provides hourly wind velocities globally on a 30-km grid resolution, in which the scatterometer and in situ wind data are assimilated to improve the accuracy of predictions (Hersbach et al. 2020). In the present study, the ERA5 winds have been analyzed to characterize the variability of hydrographic parameters.

## Results and discussion

### Comparison with Coriolis Ocean Dataset

Close to the EEZ, Copernicus data has limited drifting buoys (Fig. 1b) during Oct 2012–Sep 2013, having only sea surface temperature (SST) as given in Table 2. These buoys are away from the transect, indicating that there is a spatial data gap in the central Gulf. In addition, the CTD data also do not coincide with that of the Coriolis drifting buoys, temporally. Therefore, a quantitative comparison between the two datasets is not feasible in the context of the spatial and temporal differences. Nonetheless, we have tabulated the SST values from both the sources with the nearest available time slots to derive some inferences (Table 2).

In the EEZ of Qatar, there is a decrease in SST of the order of 2.9–4.5 °C in the EEZ of Qatar in the period between October and November. This is a transition period from summer to winter in which the shamal wind cools the sea surface faster than the inter-seasonal shifts in temperature. In addition, spatial variability exists between the west and east parts of the EEZ of Qatar (Elobaid et al. 2022). Between December and January, there is no significant temporal variation in SST. However, its spatial variability has more relevance. For instance, the drifting buoy 23,519 is the nearest Coriolis platform of Stn. 3, where the SST is only 0.3 °C higher than that of Stn.3. Stn. 6 is further offshore, where the SST is 0.9° higher than that at Stn. 3. To the west of

**Table 2** The SST values obtained from the cruises (CTD) and Coriolis (drifting buoys) datasets with the nearest available time and space slots

| Data source | Stations/Platform | SST (°C) | | | |
|---|---|---|---|---|---|
| CTD (cruise) | Stn.3 | 33.0 (04 Oct 2012) | 22.8 (09 Jan 2013) | 24.5 (12 Apr 2013) | 33.8 (31 Aug 2013) |
| | Stn.6 | 32.3 (04 Oct 2012) | 23.7 (09 Jan 2013) | 24.2 (12 Apr 2013) | 33.8 (31Aug 2013) |
| Drifting buoys (Coriolis) | 23,754 | 29.4 (13 Nov 2012) | 21.7 (02 Jan 2013) | – | – |
| | 23,749 | 28.8 (13 Nov 2012) | 21.0 (05 Jan 2013) | – | – |
| | 23,756 | 28.6 (13 Nov 2012) | 20.2 (27 Dec 2012) | – | – |
| | 23,750 | 28.6 (23 Nov 2012) | – | – | – |
| | 23,519 | 28.5 (23 Nov 2012) | 23.1 (05 Jan 2013) | – | – |
| | 23,744 | – | – | – | 33.3 (16 Sep 2013) |
| | 23,739 | – | – | – | 33.1 (16 Sep 2013) |
| | 23,741 | – | – | 22.5 (31 Mar 2013) | – |

the cruise transect (outside the EEZ), the drifting buoy data (23,754, 23,749, 23,756) has lower SST compared to Stn. 3 and Stn.6, with a decrement of the order of 2.0–3.5 °C. This spatial variation in SST is a major concern, especially when several water masses are active in the central Gulf. It has been discovered that the relatively warm water mass from the Sea of Oman during winter has a significant impact in Qatar's EEZ (Rakib et al. 2021). Between March and April, the increment in SST is evident due to an increase in solar radiation. During the end of August and September, within a short time span, the CTD and buoy SSTs show small spatial variations. The co-analysis of Coriolis data with the transects indicates the necessity of having more observations in the EEZ of Qatar to improve the understanding of the physical variables.

## Seasonal variability in hydrography and water mass distribution

The temperature, salinity, and density ($\sigma_t$) along the track connecting the sampling stations show systematic variations (Fig. 2). Horizontal and vertical variability is evident across the transect. However, they are not consistent across the seasons. The SST is relatively higher in the nearshore region during October 2012 and April 2013 with a difference of about 1.0 °C compared to the deepest station, whereas the opposite is true during January 2013, June 2013, and August 2013 with a difference of about 1.0–2.0 °C. The variation in sea surface salinity (SSS) is about 1.0–2.0 during all the seasons. The SSS is relatively higher in the nearshore region and progressively decreases towards the deepest station during all the seasons, except during August 2013. During

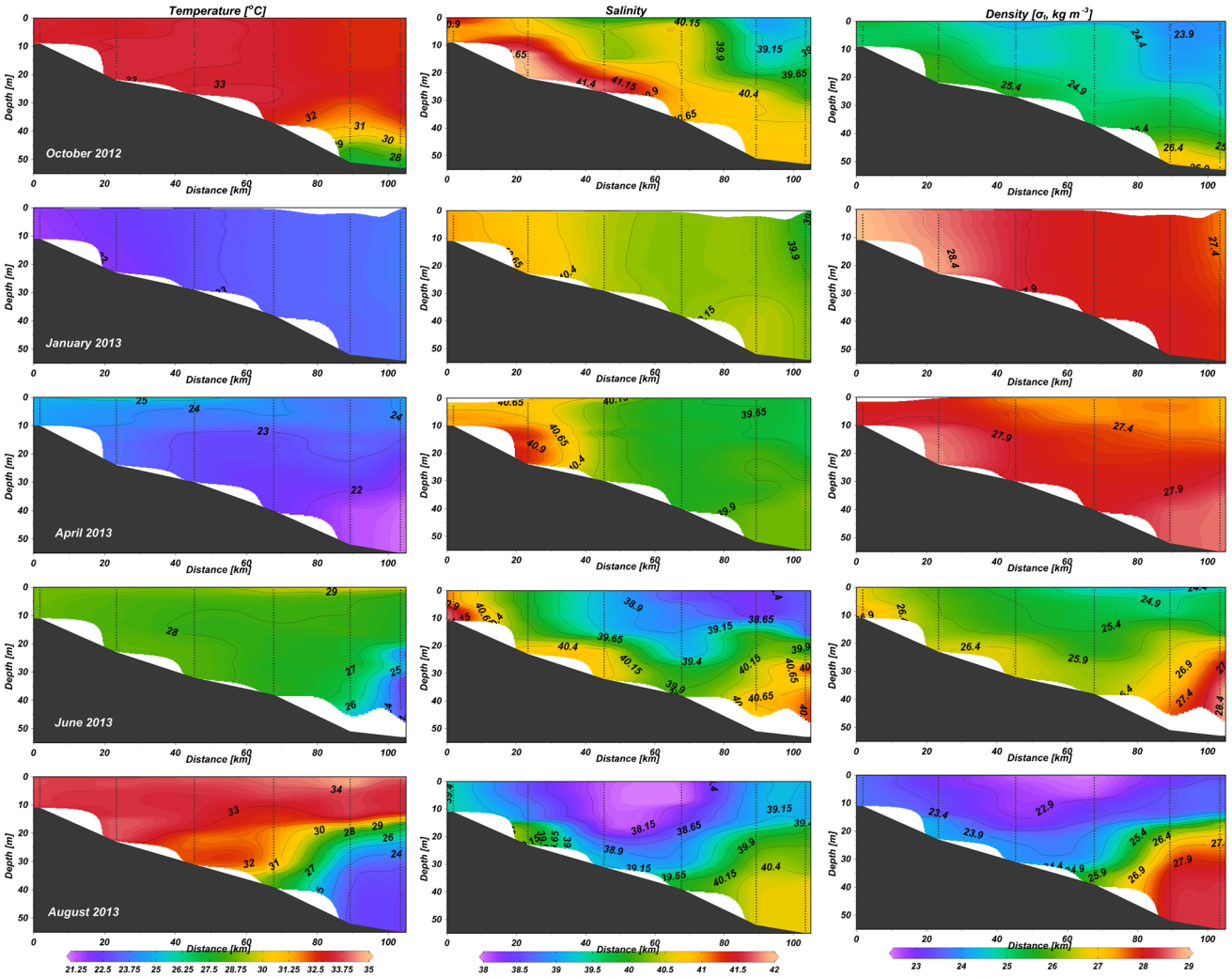


**Fig. 2** Vertical and horizontal distribution of temperature (ºC) (left), salinity (middle), and density ($\sigma_t$) (kg $m^{-3}$) (right) from station 1 to station 6 during different seasons

August 2013, the surface layer in the middle of the transect showed a lower salinity compared to the nearshore and offshore stations. This relatively fresh and low-density water inflow is caused by the IOSW. Its impact has been stretched up to the nearshore region, where the salinity has dropped to 2.0 compared to the nearshore salinity during June 2013. Elobaid et al. (2022) reported a similar nearshore-offshore gradient in SSS during late summer in a different transect beginning in the southern part of Qatar's east coast and ending in a region adjacent to Stn. 6. They reported a nearshore SSS of about 44.3, while the nearshore SSS we measured in the central nearshore region is about 42.0. Both of these locations have a distance of about 80 km apart. Thus, the dynamics that lead to the difference in nearshore salinity are quite different. The wind mixing and the proximity to the deep waters of the central Gulf are relatively higher on the central east coast compared to the southern east coast, which enables a relatively faster mixing of SSS with the adjacent regions. It is also linked with the influence of brine discharges from the desalination plants (Elobaid et al. 2022; Rakib et al. 2021).

Hypersaline and relatively colder water formed in the nearshore region cascades downslope from January 2012 through April 2013. During summer and fall, the formation of high-saline deep-water masses and the intrusion of low-salinity water from the Sea of Oman into the surface layer appear as counter-acting processes. The low-saline surface layer appears only in the offshore area during summer (June 2013), which has a thickness of about 15 m. During late summer (August 2013), the layer moves shoreward and deepens down to about 20 m due to a downwelling cell, which is associated with an anti-cyclonic eddy formed in the central Gulf between two cyclonic eddies (Thoppil and Hogan 2010). During the fall (October 2012), only a modified remnant of the intrusion layer is observed offshore.

The temperature variability of the whole surface layer in the study area is minimal down to about 20-m depth in all seasons, excluding late summer when a strong thermocline is formed offshore (Fig. 3). The vertical temperature distribution in the offshore is mainly controlled by the seasonal mixing-stratification cycle. The water column is vertically homogenous during January 2013. Atmospheric cooling and wind-induced mixing during the winter collectively produce a homogenous water column in the Gulf (Thoppil and Hogan 2010; Al Azhar et al. 2016). The daily average wind speed during January 2013 goes up to 11.7 m/s in the offshore (station 6), while the monthly average wind speed is 4.6 m/s (Fig. 4). The seasonal thermocline forms during early summer (June 2013, 22 m) and strengthens throughout the season (August 2013, 15 m). From April through August, the water below 30 m depth is cooler than that during January, showing the effect of thermal isolation on the summer bottom layer. The pycnocline is stronger during late summer (August 2013), and this corresponds to a density difference of about 3.5 kg $m^{-3}$ between 12 and 25 m water depths (Fig. 3c). As surface warming continues through October, the seasonal thermocline and halocline weaken and deepen (Fig. 3a, b). This is aligned with a weakening of low-salinity surface inflow. As the atmospheric heating is sustained into the fall season (October 2012), atmospheric warming extends to deeper depths; thus, the thermocline deepens below 40 m. This is consistent with the thermocline obtained in the deep water of the central transect during late September in a previous investigation (Elobaid et al. 2022; Rakib et al. 2021).

The potential temperature-salinity (Θ/S) diagram (Fig. 5) shows a clear seasonal variability in water mass characteristics. Salinity (37.99–41.65) and density (22.49–28.66 kg $m^{-3}$) ranges are narrower than temperature (21.04–34.63 °C). It is inferred that salinity is the

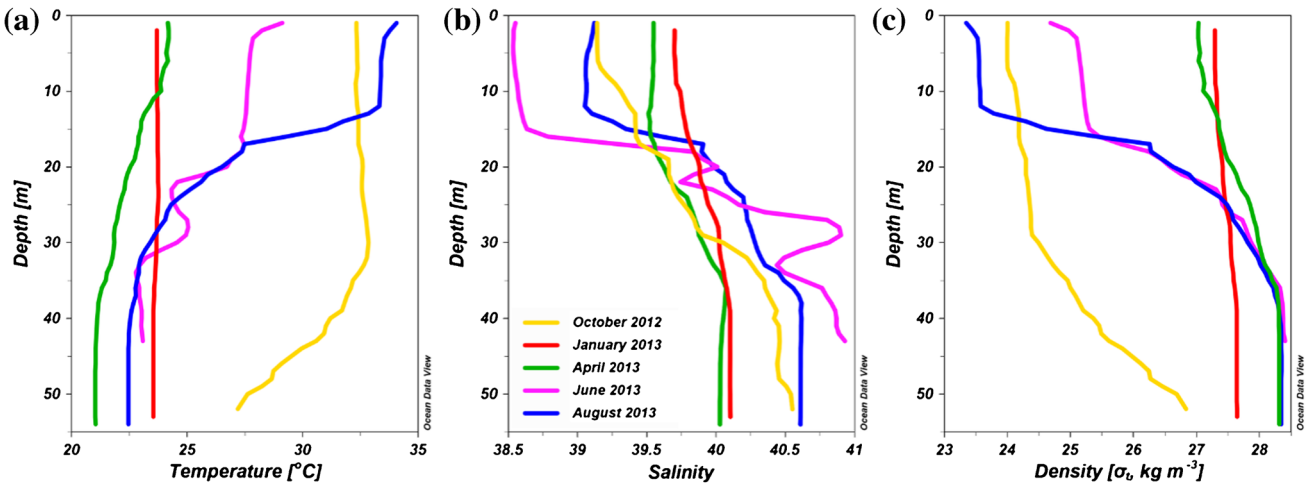


**Fig. 3** Vertical profiles of **a** temperature (ºC), **b** salinity, and **c** density ($\sigma_t$) (kg $m.^{-3}$) for all cruises at the deepest sampling station (station 6)

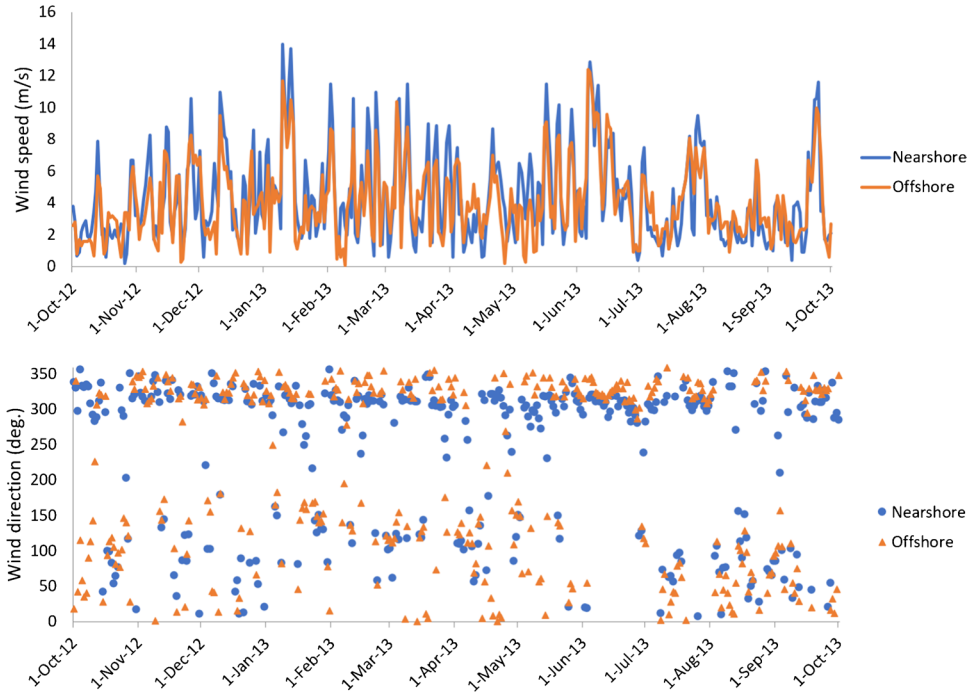


**Fig. 4** Daily average wind speed in the nearshore (station 1) and offshore (station 6) locations during October 2012–September 2013

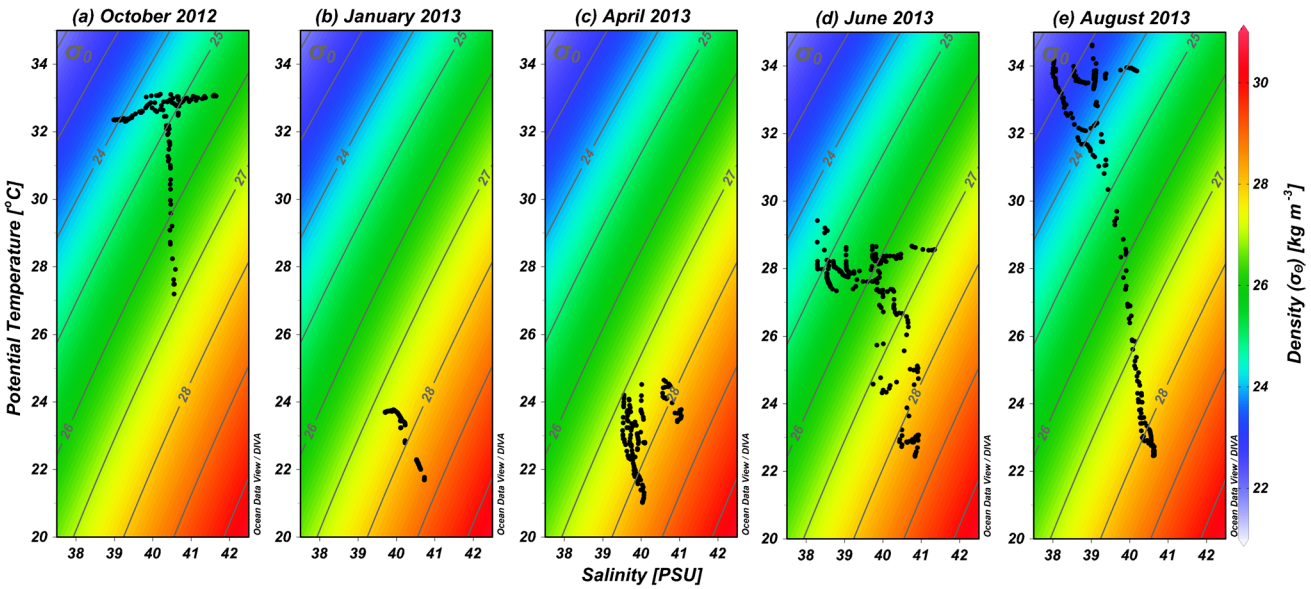


**Fig. 5** Θ/S diagrams during **a** October 2012, **b** January 2013, **c** April 2013, **d** June 2013, and **e** August 2013 at stations 1 to 6. Black dots indicate the potential densities. Contour lines represent isopycnals (kg m.$^{-3}$)

main contributor to the variability in density. However, the temperature does have robust links during the transition periods. Vigorous vertical mixing due to the combined effects of decreased insolation, high wind speeds, and enhanced convection confines winter water masses to a small range of densities ($\sigma_t$: 27.30–28.66 kg m$^{-3}$). The range of densities is relatively wider in summer ($\sigma_t$: 22.49–28.37 kg m$^{-3}$), which is driven by the warming and freshening of the surface layer. Similar seasonal variations are identified in the earlier studies in the central Gulf (Al-Ansari 2006; Hassan and Mahmoud 1986; Rakib et al. 2021). The extent of low salinity (< 40) surface waters of Sea of Oman origin is particularly pronounced during the summer and to a lesser extent during the winter, consistent

with earlier observations (Al-Shehhi et al. 2021; Campos et al. 2020). Offshore, deep waters below 30 m in the EEZ of Qatar remain colder and saltier throughout the summer, as vertical convection is hindered by seasonal pycnocline. By early fall (October), stratification has weakened considerably, rendering deeper waters warmer and relatively fresher than in summer.

### Variability of DO and chlorophyll fluorescence

Distinct seasonal variability is observed in the DO concentration along the transect (Fig. 6). In October 2012, the surface layer has a DO of above 125 µmol $l^{-1}$, while the bottom layer (below 50 m) has a lesser DO, on the border of hypoxia. On the other hand, hypoxia is evident below 40-m depth during August 2013. However, it is not evident during June 2013. Earlier, Al-Ansari et al. (2015) identified hypoxic conditions in the deeper water of the EEZ of Qatar during September. These indicate that the hypoxia in the EEZ of Qatar is intra-seasonal and occurs in the late summer, explicitly during August–September. The stratification of offshore waters by excessive surface heating (Elobaid et al. 2022; Mosaddad et al. 2012), dense and relatively cold deep water flow originating from the northern Gulf (Al Azhar et al. 2016), and relatively calm wind conditions (Fig. 4) together catalyzes the biogeochemical interactions leading to hypoxia. Weakening of stratification during October 2012 (Fig. 2) enabled the deep waters to make a slow recovery from the hypoxic conditions, and strong mixing during winter enriched the DO to a healthy level through the spring. The overall maxima in DO (> 201 µmol $l^{-1}$ at about 100% saturation) are observed during April 2013 in the offshore surface layer, during which the water column in the offshore is well mixed. Although hypoxia exists in the deeper depths of the offshore region during August 2013, the surface layer in the middle of the transect is augmented with sufficient DO, of about 175 µmol $l^{-1}$. This is aligned with a relatively fresh and low-density surface water inflow (Fig. 2), caused by the IOSW.

The chlorophyll fluorescence measured during three cruises indicates that the overall phytoplankton biomass is low to moderate during April 2013 and June 2013 and relatively high during August 2013 (Fig. 7). Laterally, the surface layer up to 10 m depth has no significant variability between the stations and the seasons, where the chlorophyll fluorescence is below 1.0 µg $l^{-1}$. The subsurface layer (between 10 and 40 m depths) shows seasonal variation, with the lowest chlorophyll fluorescence (~ 1.0 mg $l^{-1}$) in April 2013, moderate in June 2013 (~ 1.5 mg $l^{-1}$), and relatively high in August 2013 (~ 6.0 mg $l^{-1}$). The highest chlorophyll fluorescence was found in Stn. 2 around 20 m, followed by ~ 3.0 µg $l^{-1}$ chlorophyll fluorescence at 20-m depth in station 6. Patches of moderate chlorophyll fluorescence can also be seen in the subsurface layer between the two stations mentioned above in August 2013. Rakib et al. (2021) identified a relatively higher chlorophyll concentration in the surface and sub-surface layers at an offshore station (adjacent to Stn. 6) during September 2014. However, early summer data measured during May 2016 (Elobaid et al. 2022) adjacent to Stn. 6 indicates a lower chlorophyll concentration, which lies in between the values obtained during April 2013 and June 2013 in the present study. This indicates that there is a gradual increase in chlorophyll fluorescence from spring to late summer. The highest chlorophyll fluorescence measured is aligned with the highest DO at the same depth during August 2013 (Fig. 6). This ensures sufficient biomass production during the late summer in the subsurface layer.

The chlorophyll fluorescence data during winter is very limited in the EEZ of Qatar. Rakib et al. (2021) measured a slightly higher concentration (~ 5.6 µg $l^{-1}$) in the offshore region of Qatar's EEZ in January 2015. Together with our observations, we can infer that the winter and late summer have relatively higher chlorophyll fluorescence in the EEZ of Qatar, while the spring and early summer have lower concentrations. The central Gulf is one of the phytoplankton abundant regions in the Gulf during winter, which is related to the circulation patterns (Polikarpov et al. 2016). This seasonal abundance is also consistent with the observations in the northern Gulf, especially in the Kuwait waters, since winter is characterized by well-oxygenated and nutrient-rich waters in this region (Ahmed et al. 2022). A more detailed investigation is required to investigate the temporal and spatial variability of the chlorophyll fluorescence and its impact on the productivity in the EEZ of Qatar.

## Summary and conclusions

Seasonal variability in temperature, salinity, density, dissolved oxygen, and chlorophyll fluorescence along a transect from nearshore to offshore in the eastern part of the EEZ of Qatar has been investigated. The sea surface temperature varies from nearshore to offshore with a positive gradient during January, June, and August, of the order of 1.0–2.0 °C, and with a negative gradient during October and April, of the order of 1.0 °C. Thermal stratification began in June, attained a well-defined thermocline with a vertical difference in temperature of about 10 °C during August, and started to de-stratify during October.

The nearshore region has the highest salinity compared to the offshore with an increment of about 2.0 in all the seasons except August. The late summer is characterized by an inflow of a relatively fresh and low-density water

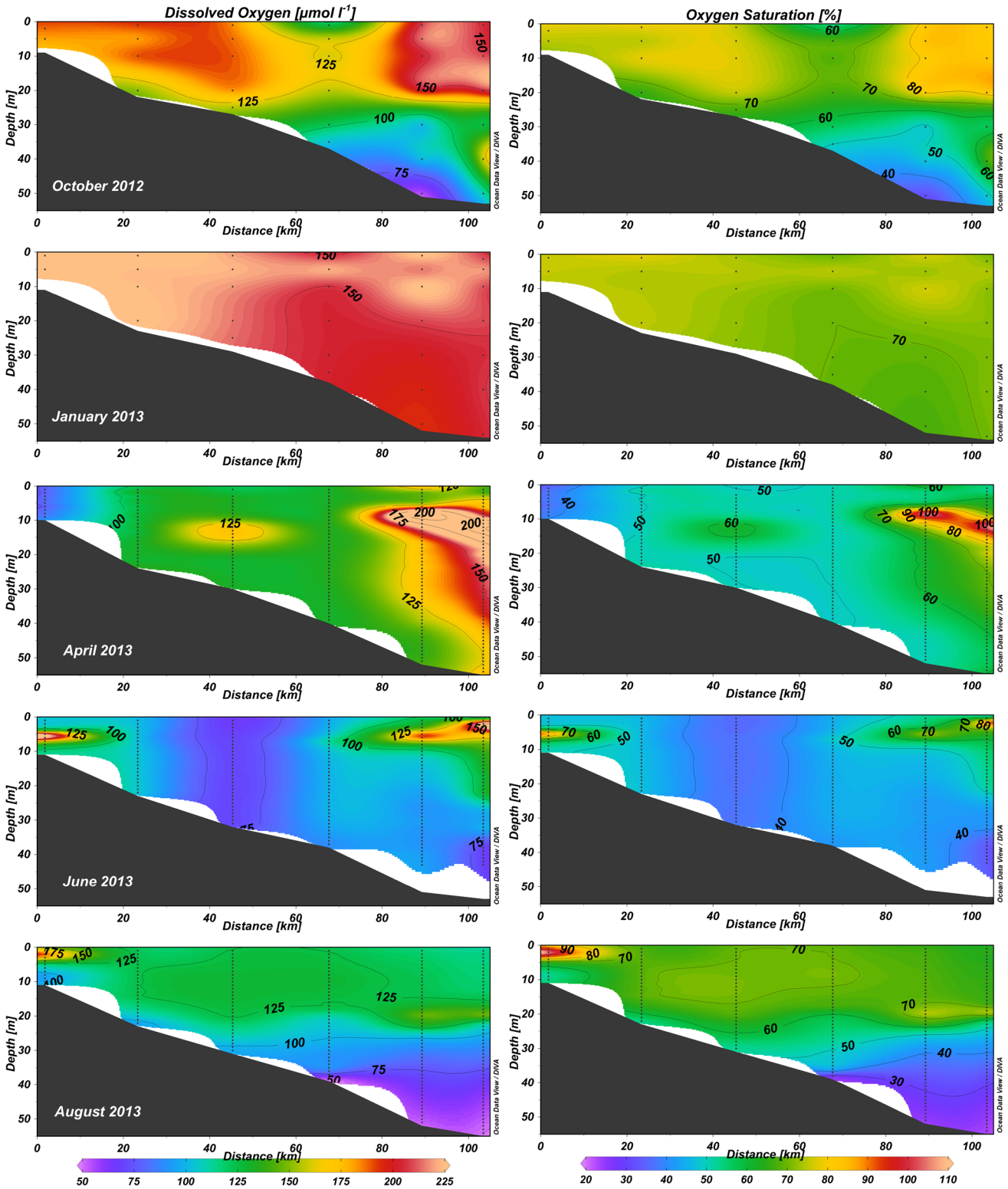


**Fig. 6** Vertical and horizontal distribution of DO concentration (µmol $l.^{-1}$) (left) and DO saturation (%) (right) from station 1 to station 6

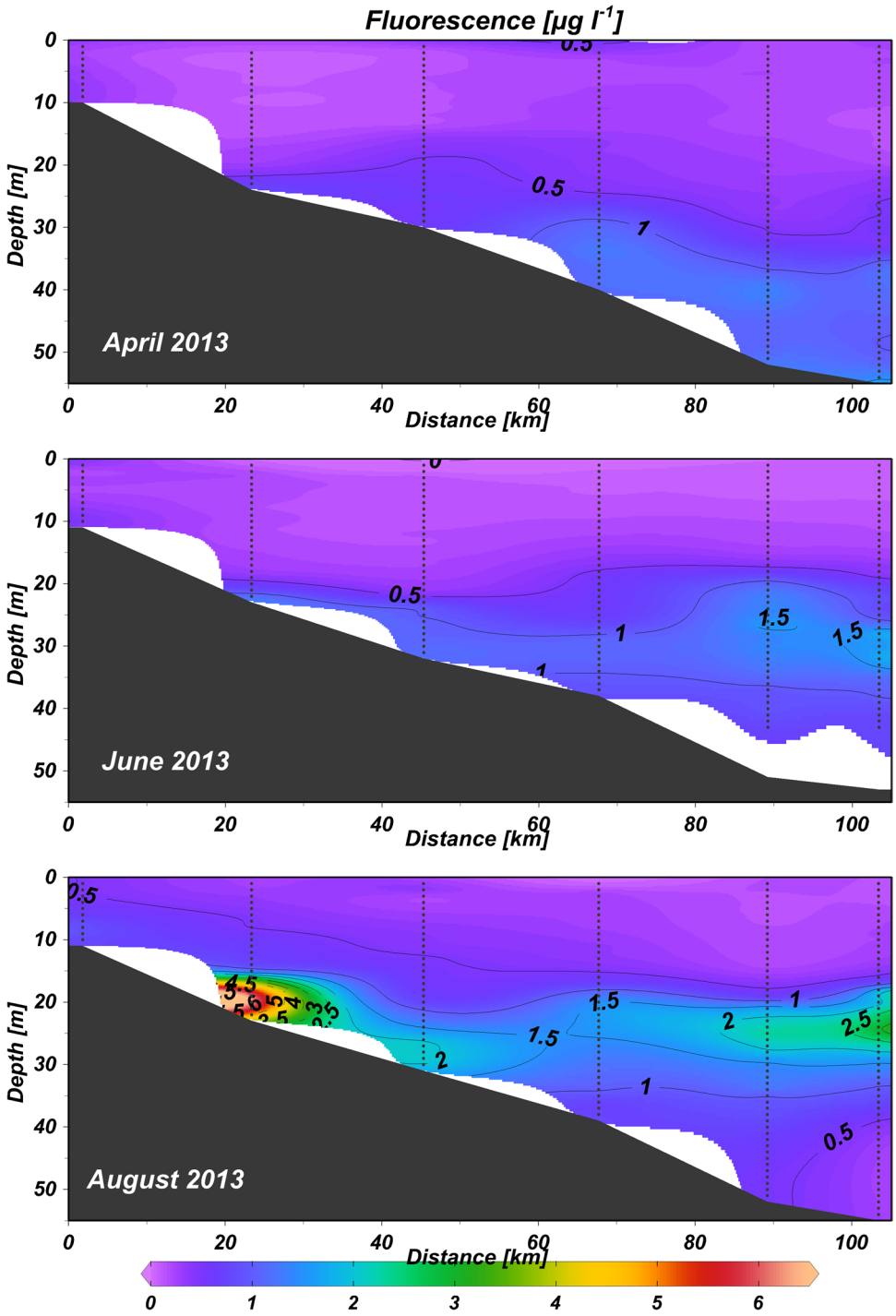


**Fig. 7** Cross-sections of chlorophyll fluorescence (µg $l^{-1}$) with cruise months indicated on the left

mass through the surface layer of the intermediate offshore stations of the transect, which has freshened the nearshore waters with a decrement of about 2.0 compared to other seasons. This substantiates the influence of the IOSW in the EEZ of Qatar, as is also evident from recent studies (Elobaid et al. 2022; Rakib et al. 2021). This surface flow has enriched the surface layer (of about 20 m) dissolved oxygen in the middle of the transect with a concentration up to 175 µmol $l^{-1}$ during August, from a concentration of about 75 µmol $l^{-1}$ during June. While hypoxia is evident in deeper depths (below 50 m) of the offshore station during August, earlier studies (Elobaid et al. 2022; Al-Ansari et al. 2015) reported hypoxia during September. Our analysis does not show hypoxia during June, and there are no

datasets available during July in the EEZ of Qatar. Hence, this study infers that the hypoxia in the EEZ of Qatar evolves in the middle of summer and is prevalent during late summer (August–September), which subsequently disappears during October. The stratification of offshore waters by excessive surface heating, dense and relatively cold deep-water flow originating from the northern Gulf and relatively calm wind conditions together play a role in the evolution and existence of hypoxia in the EEZ of Qatar.

The surface layer up to 10-m depth has lower chlorophyll fluorescence (below 1.0 μg $l^{-1}$) from April to August, whereas the sub-surface layer (between 10 and 40 m depths) has distinct seasonal variability, with the lowest chlorophyll fluorescence in April 2013 (~ 1.0 μg $l^{-1}$), moderate in June 2013 (~ 1.5 μg $l^{-1}$), and relatively high in August 2013 (~ 6.0 μg $l^{-1}$). The chlorophyll fluorescence data during winter is very limited in the EEZ of Qatar. Together with earlier observations, we can deduce that the winter and late summer have relatively higher chlorophyll fluorescence in the EEZ of Qatar, while the spring and early summer have lower concentrations. Obvious in situ data gaps still exist in the EEZ of Qatar, which need to be filled with more observations in future studies. Further studies on phytoplankton species distribution, nutrient concentrations, and flow dynamics are currently underway for a more comprehensive understanding of the coupled physical-biogeochemical dynamics of the EEZ of Qatar.

**Acknowledgements** The authors would like to thank the Environmental Science Center (ESC) and Department of Biological and Environmental Sciences (DBES), College of Arts and Sciences, Qatar University for ship-time and facilities provided for the study. We also would like to thank the research and technical staff of ESC and DBES, and the Captain and crew of R/V Janan for fieldwork and laboratory analyses. This work has been supported by the QAFCO project (Grant no. QUEX-ESC-QAFCO-20/21-2). The open access funding of this article is provided by the Qatar National Library.

**Author contribution** Ebrahim Al-Ansari: conceptualization, formal analysis, funding acquisition, investigation, methodology, project administration, resources, supervision, writing — original draft; Yusuf Sinan Husrevoglu: conceptualization, data curation, formal analysis, investigation, methodology, resources, software, visualization, writing — original draft; Oguz Yigiterhan: conceptualization, data curation, formal analysis, investigation, project administration, resources, supervision, visualization, writing — original draft; Nabiha Youssef: conceptualization, data curation, formal analysis, investigation, methodology, software, visualization, writing — original draft; Ibrahim A. Al-Maslamani: conceptualization, data curation, formal analysis, methodology, writing — original draft; Mohamed A. Abdel-Moati: conceptualization, data curation, formal analysis, methodology, writing — original draft; Ahmad J. Al-Mohamedi: data curation, formal analysis, methodology, software, writing — original draft; Valliyil Mohammed Aboobacker: conceptualization, formal analysis, investigation, methodology, supervision, writing – review and editing; Ponnumony Vethamony: conceptualization, funding acquisition, investigation, methodology, supervision, writing — review and editing.

**Funding** Open Access funding provided by the Qatar National Library.

## Declarations

**Conflict of interest** The authors declare no competing interests.

**Open Access** This article is licensed under a Creative Commons Attribution 4.0 International License, which permits use, sharing, adaptation, distribution and reproduction in any medium or format, as long as you give appropriate credit to the original author(s) and the source, provide a link to the Creative Commons licence, and indicate if changes were made. The images or other third party material in this article are included in the article's Creative Commons licence, unless indicated otherwise in a credit line to the material. If material is not included in the article's Creative Commons licence and your intended use is not permitted by statutory regulation or exceeds the permitted use, you will need to obtain permission directly from the copyright holder. To view a copy of this licence, visit http://creativecommons.org/licenses/by/4.0/.

## References

Aboobacker VM, Shanas PR, Veerasingam S, Al-Ansari IMAS, Sadooni FN, Vethamony P (2021a) Long-term assessment of onshore and offshore wind energy potentials of Qatar. Energies 14:1178

Aboobacker VM, Shanas PR, Veerasingam S, Al-Ansari IMAS, Sanil Kumar V, Vethamony P (2021b) The maxima in northerly wind speeds and wave heights over the Arabian Sea, the Arabian/Persian Gulf and the Red Sea derived from 40 years of ERA5 data. Clim Dyn 56:1037–1052

Aboobacker VM, Samiksha SV, Veerasingam S, Al-Ansari IMAS, Vethamony P (2021c) Role of shamal and easterly winds on the wave characteristics off Qatar, central Arabian Gulf. Ocean Eng 236:109457

Ahmed A, Madhusoodhanan R, Yamamoto T, Fernandes L, Al-Said T et al (2022) Analysis of phytoplankton variations and community structure in Kuwait Bay, Northwestern Arabian Gulf. J Sea Res 180:102163

Al-Mutairi N, Abahussain A, El-Battay A (2014) Application of water quality index to assess the environmental quality of Kuwait Bay. International Conference on Advances in Agriculture, Biological & Environmental Sciences (AABES-2014), Oct 15–16, 2014, Dubai, UAE, pp 1–5

Al Senafi F, Anis A (2015) Shamals and climate variability in the Northern Arabian/Persian Gulf from 1973 to 2012. Int J Climatol 35:4509–4528

Al-Ansari IMAS, Rowe G, Abdel-Moati MAR, Yigiterhan O, Al-Maslamani I, Al-Yafei MA, Al-Shaikh I, Upstill-Goddard R (2015) Hypoxia in the central Arabian Gulf Exclusive Economic Zone (EEZ) of Qatar during summer season. Estuar Coast Shelf Sci 159:60–68

Al-Ansari IMAS (2006) A hydrographic and biogeochemical study of waters and sediment of the exclusive economic zone (EEZ) of Qatar (Arabian Gulf). Ph.D. thesis. The University of Newcastle Upon Tyne, UK

Al-Ansi MA, Abdel-Moati MAR, Al-Ansari IMAS (2002) Causes of fish mortality along the Qatari Waters (Arabian Gulf). Int J Environ Stud 59:59–71

Al Azhar M, Temimi M, Zhao J, Ghedira H (2016) Modeling of circulation in the Arabian Gulf and the Sea of Oman: skill assessment and seasonal thermohaline structure. J Geophys Res (oceans) 121:1700–1720

Al-Mazroui M, Islam MN, Jones PD, Athar H, Rahman MA (2012) Recent climate change in the Arabian Peninsula: seasonal rainfall and temperature climatology of Saudi Arabia for 1979–2009. Atmos Res 111:29–45

Al-Naimi N, Raitsos D, Ben-Hamadou R, Soliman Y (2017) Evaluation of satellite retrievals of chlorophyll-a in the Arabian Gulf. Remote Sens 9:301

Al-Qaradawi I, Abdel-Moati M, Al-Yafei M et al (2015) Radioactivity levels in the marine environment along the exclusive economic zone (EEZ) of Qatar. Mar Pollut Bull 90:323–329

Al-Shehhi MR, Song H, Scott J, Marshall J (2021) Water mass transformation and overturning circulation in the Arabian Gulf. J Phys Oceanogr 51:3513–3527

Al-Yamani F, Naqvi SWA (2019) Chemical oceanography of the Arabian Gulf. Deep Sea Res Part II 161:72–80

Azizpour J, Chegini V, Khosravi M, Einali A (2014) Study of the physical oceanographic properties of the Persian Gulf, Strait of Hormuz and Gulf of Oman based on PG-GOOS CTD measurements. J Persian Gulf 5(18):37–48

Campos EJD, Gordon AL, Kjerfve B, Vieira F, Cavalcante G (2020) Freshwater budget in the Persian (Arabian) Gulf and exchanges at the Strait of Hormuz. PLoS ONE 15(5):e0233090

de Verneil A, Burt JA, Mitchell M, Paparella F (2021) Summer oxygen dynamics on a Southern Arabian Gulf Coral Reef. Front Mar Sci 8:781428

Elobaid EA, Al-Ansari EMAS, Yigiterhan O, Aboobacker VM, Vethamony P (2022) Spatial variability of summer hydrography in the central Arabian Gulf. Oceanologia 64:75–87

Feary DA, Burt JA, Bartholomew A (2011) Artificial marine habitats in the Arabian Gulf: review of current use, benefits and management implications. Ocean Coast Manag 54:742–749

Hassan HM, Mahmoud MA (1986) Hydrography of the Western Part of the Arabian Gulf. Qatar Univ Sci Bull 6:349–362

Hersbach H, Bell B, Berrisford P, Hirahara S, Horányi A, Muñoz-Sabater J, Nicolas J, Peubey C, Radu R, Schepers D et al (2020) The ERA5 global reanalysis. Q J R Meteorol Soc 146:1999–2049

Hosseini H, Saadaoui I, Moheimani N, Al Saidi M, Al Jamali F, Al Jabri H, Ben Hamadou R (2021) Marine health of the Arabian Gulf: drivers of pollution and assessment approaches focusing on desalination activities. Mar Pollut Bull 164:112085

Ibrahim HD, Xue P, Eltahir EAB (2020) Multiple salinity equilibria and resilience of Persian/Arabian gulf basin salinity to brine discharge. Front Mar Sci 7:573. https://doi.org/10.3389/fmars.2020.00573

Janzen C, Larson N, Murphy D (2008) Long-Term Oxygen Measurements. Sea-Bird Electronics, Inc. International Ocean Systems 12(2). http://archive.ssc-ras.ru/eg/Equipment/SBE_19plusV2/website/technical_references/IOS43Article-MarApr2008.htm. Accessed March/April 2008

Johns WE, Yao F, Olson DB, Josey SA, Grist JP, Smeed DA (2003) Observations of seasonal exchange throughthe Straits of Hormuz and the inferred heat and freshwater budgets of the Persian Gulf. J Geophys Res 108(C12):3391. https://doi.org/10.1029/2003JC001881

Jones DA (1985) The biological characteristics of the marine habitats found within the ROPME Sea Area. Proceedings of ROPME Symposium on Regional Marine Pollution Monitoring and Research Programmes, ROPME/GC-4/2 (1985), pp 71–89

Joydas TV, Qurban MA, Manikandan KP, Ashraf TTM, Ali SM, Al-Abdulkader K, Qasem A, Krishnakumar PK (2015) Status of macrobenthic communities in the hypersaline waters of the Gulf of Salwa. Arabian Gulf J Sea Res 99:34–46. https://doi.org/10.1016/j.seares.2015.01.006

Kampf J, Sadrinasab M (2006) The circulation of the Persian Gulf: a numerical study. Ocean Sci 2:27–41

Lachkar Z, Lévy M, Smith KS (2019) Strong intensification of the Arabian Sea oxygen minimum zone in response to Arabian Gulf warming. Geophys Res Lett 46:5420–5429

L'Hégaret P, de Marez C, Morvan M, Meunier T, Carton X (2021) Spreading and vertical structure of the Persian Gulf and Red Sea outflows in the Northwestern Indian Ocean. J Geophys Res Oceans 126. https://doi.org/10.1029/2019JC015983

Lorenz M, Klingbeil K, Burchard H (2020) Numerical study of the exchange flow of the Persian Gulf using an extended total exchange flow analysis framework. J Geophys Res Oceans 125:e2019JC015527

Mezhoud N, Temimi M, Zhao J, Al Shehhi MR, Ghedira H (2016) Analysis of the spatio-temporal variability of seawater quality in the southeastern Arabian Gulf. Mar Pollut Bull 106:127–138

Mosaddad SM, Bidokhti AA, Basirparsa H (2012) An observational and numerical modeling of thermocline development in the Persian Gulf. Mar Geod 35:32–48

Naqvi SWA (2021) Deoxygenation in Marginal Seas of the Indian Ocean. Front Mar Sci 8.https://doi.org/10.3389/fmars.2021.624322

Noori R, Tian F, Berndtsson R, Abbasi MR, Naseh MV, Modabberi A, Soltani A, Kløve B (2019) Recent and future trends in sea surface temperature across the Persian Gulf and Gulf of Oman. PLoS ONE 14(2):e0212790

Perrone TJ (1979) Winter shamal in the Persian Gulf. Naval Environmental Prediction Research Facility, Technical Report, Monterey, CA, p 180

Polikarpov I, Saburova M, Al-Yamani F (2016) Diversity and distribution of winter phytoplankton in the Arabian Gulf and the Sea of Oman. J Coastal Res 119:85–99

Pous S, Lazure P, Carton X (2015) A model of the general circulation in the Arabian Gulf and in the Strait of Hormuz: Intraseasonal to interannual variability. Cont Shelf Res 94:55–70. https://doi.org/10.1016/j.csr.2014.12.008

Quigg A, Al-Ansi M, Al Din NN et al (2013) Phytoplankton along the coastal shelf of an oligotrophic hypersaline environment in a semi-enclosed marginal sea: Qatar (Arabian Gulf). Cont Shelf Res 60:1–16

Rakib MF, Al-Ansari EMAS, Husrevoglu S, Yigiterhan O, Al-Maslamani IA, Aboobacker VM, Vethamony P (2021) Observed variability in physical and biogeochemical parameters in the central Arabian Gulf. Oceanologia 63:227–237

Reynolds RM (1993) Physical oceanography of the Gulf, Strait of Hormuz, and the Gulf of Oman—Results from the Mt Mitchell expedition. Mar Pollut Bull 27:35–59

Sadrinasab M, Kämpf J (2004) Three-dimensional flushing times of the Persian Gulf. Geophys Res Lett 31:L24301

Saleh A, Abtahi B, Mirzaei N, Chen CTA, Ershadifar H, Ghaemi M, Hamzehpour A, Abedi E (2021) Hypoxia in the Persian Gulf and the Strait of Hormuz. Mar Pollut Bull 167:112354

Schlitzer R (2015) Data analysis and visualization with Ocean Data View. CMOS Bulletin SCMO 43:9–13

Sheehan PMF, Webber BGM, Sanchez-Franks A, Matthews AJ, Heywood KJ, Vinayachandran PN (2020) Injection of oxygenated Persian Gulf water into the Southern Bay of Bengal. Geophys Res Lett 47:e2020GL087773

Sheppard C, Al-Husiani M, Al-Jamali F et al (2010) The Gulf: a young sea in decline. Mar Pollut Bull 60:13–38

Strong AE, Liu G, Skirving W, Eakin CM (2011) NOAA's coral reef watch program from satellite observations. Ann GIS 17(2):83–92

Swift SA, Bower AS (2003) Formation and circulation of dense water in the Persian/Arabian Gulf. J Geophys Res 108:3004

Tanguy S, Jerome G, Sylvie P, Gilles R (2019) CORA, Coriolis Ocean Dataset for Reanalysis. SEANOE. https://doi.org/10.17882/46219

Thoppil PG, Hogan PJ (2010) Persian Gulf response to a wintertime shamal wind event. Deep Sea Res. Part I Oceanogr Res Pap 57:946–955

Veerasingam S, Al-Khayat JA, Aboobacker VM, Hamza S, Vethamony P (2020a) Sources, spatial distribution and characteristics of marine litter along the west coast of Qatar. Mar Pollut Bull 159:111478

Veerasingam S, Al-Khayat JA, Haseeba KP, Aboobacker VM, Hamza S, Vethamony P (2020b) Spatial distribution, structural characterization and weathering of tarmats along the west coast of Qatar. Mar Pollut Bull 159:111486

Winkler LW (1888) Die Bestimmung des im Wasser gelösten Sauerstoffes. Berichte Der Dtsch Chem Gesellschaft 21:2843–2854

Xue P, Eltahir EAB (2015) Estimation of the heat and water budgets of the Persian (Arabian) Gulf using a regional climate model. J Clim 28:5041–5062

Yao F, Johns WE (2010a) A HYCOM modeling study of the Persian Gulf: 1. Model configurations and surface circulation. J Geophys Res 115:C11017

Yao F, Johns WE (2010b) A HYCOM modeling study of the Persian Gulf: 2. Formation and export of Persian Gulf Water. J Geophys Res 115:C11018